Inorganic Chemistry

Article

pubs.acs.org/IC

Anion Encapsulation and Geometric Changes in Hepta- and Hexanuclear Copper(I) Dichalcogeno Clusters: A Theoretical and Experimental Investigation

Camille Latouche,[†] Samia Kahlal,[†] Yan-Ru Lin,[‡] Jian-Hong Liao,[‡] Eric Furet,[†] C. W. Liu,*[,‡] and Jean-Yves Saillard*[,†]

[†]Institut des Sciences Chimiques de Rennes, UMR 6226 CNRS-Université de Rennes 1-Ecole Nationale Supérieure de Chimie de Rennes, Avenue du Général Leclerc, 35042 Rennes, France

[‡]Department of Chemistry, National Dong Hwa University, Hualien, Taiwan 97401, Republic of China

Supporting Information

ABSTRACT: Whereas stable octanuclear clusters of the type $M^I_8(E^{\cap}E)_6$ (M = Cu, Ag; $E^{\cap}E$ = dithio or diseleno ligand) are known for being able to encapsulate a hydride or main-group anion under some circumstances, only the related hydride-containing heptanuclear $[M^I]_7(H)(E^{\cap}E)_6$ and empty hexanuclear $[M^I]_6(E^{\cap}E)_6$ species have been characterized so far. In this paper we investigate by the means of theoretical calculations and experiments the viability of empty and anion-centered clusters of the type $[Cu^I]_7(X)(E^{\cap}E)_6$ and $[Cu^I]_6(X)(E^{\cap}E)_6$ (X = vacancy, H or a main-group atom). The theoretical prediction for the existence of anion-containing heptanuclear species, the shape of which is modulated by the anion nature and size, have been fully confirmed by the synthesis and characterization of $[Cu_7(X)\{S_2P(O^iPr)_2\}_6]$ (X = H, Br). This consistency between experiment and theory allows us to predict the stability and shape-modulated structure of a whole series of $[Cu^I]_7(X)(E^{\cap}E)_6$ (X = vacancy, H, O, S, halogen) and $[Cu^I]_6(X)(E^{\cap}E)_6$ (X = H, halogen) clusters.

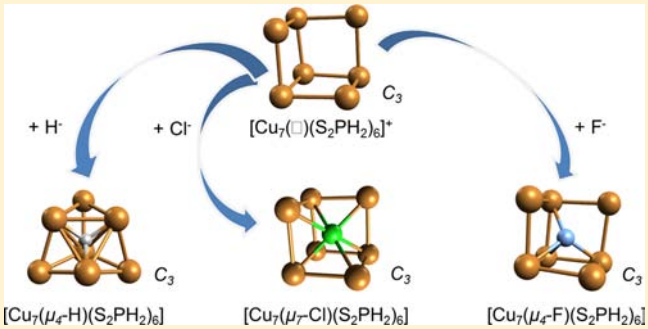

INTRODUCTION

Cu^I and Ag^I are known for forming with dithio or diseleno ligands various types of clusters, among which the octanuclear cationic family $[M^I]_8(E^{\cap}E)_6$ (M = Cu, Ag; $E^{\cap}E$ = dithio or diseleno ligand) is well documented.[1,2] Such cubic cages are rather flexible, since there is no formal metal−metal bonding, only a weak d^{10}−d^{10} interaction. On the other hand, the existence of accepting orbitals on the 16-electron metal centers allows these octanuclear cages to entrap, under certain conditions, various types of main-group anions as well as hydride.[2−7] We have shown that the incorporation of hydride distorts the cubic cage into a tetracapped tetrahedron (Scheme 1).[5−7] Such a tetrahedral distortion also occurs upon incorporation of oxide and fluoride, but it is weaker in the case of oxide and very weak in the case of fluoride.[5a,c]

On the other hand, heptanuclear species with the same number of $E^{\cap}E$ ligands have been recently characterized. All contain an encapsulated hydride.[8] These compounds, namely $Cu_7(H)(S_2CR)_6$ (R = NPr_2, NEt_2, aza-15-crown-5)[8a] and $Ag_7(H)[E_2P(OR)_2]_6$ (E = S, Se; R = ^{i}Pr, Et),[8b] exhibit a tricapped-tetrahedral shape. They can be generated from their octanuclear tetracapped-tetrahedral hydride relatives by elimination of one M^I capping atom upon reaction with BH_4^- (Scheme 1). Interestingly, hexanuclear species, still with the same number of ligands, i.e., $[M^I]_6(E^{\cap}E)_6$ clusters, are also known ($Cu_6[S_2P(OEt)_2]_6$,[4c] $Ag_6[Se_2P(O^iPr)_2]_6$,[4d] $Ag_6[S_2P(O^iPr)_2]_6$[9a]). To our knowledge, no anion incorporation inside these hexanuclear cages stabilized by dichalcogeno ligands has been reported so far.

Scheme 1. Tetracapped-Tetrahedral Octanuclear and Tricapped-Tetrahedral Heptanuclear Clusters Encapsulating Hydride

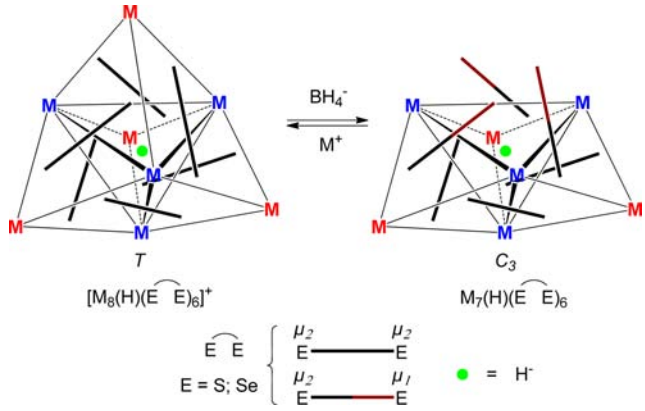

Received: August 29, 2013
Published: October 30, 2013

   dx.doi.org/10.1021/ic402207u | Inorg. Chem. 2013, 52, 13253−13262

In this paper, we investigate the possibility of existence of heptanuclear $[M^I]_7(E^{\cap}E)_6$ empty cages as well as their potential ability for encapsulating main-group atoms. We also explore the possibility of some of the known hexanuclear $[M^I]_6(E^{\cap}E)_6$ cages for encapsulating anions. The investigated systems are of the type $[Cu_7(E_2PR_2)_6]^+$ and $Cu_6(E_2PR_2)_6$ (E = S, Se; R = H, O^{i}Pr) and the resulting species after encapsulation of hydride and various saturated main-group anions.

COMPUTATIONAL DETAILS

DFT calculations have been carried out on $[Cu_7(X)(E_2PH_2)_6]^q$ and on $[Cu_6(X)(E_2PH_2)_6]^{q-1}$ (E = S, Se; X = □ (vacancy), q = +1; X = H, F, Cl, Br, q = 0; X = O, S, Se, q = −1) with the Gaussian 09 package.[10] The BP86 functional[11] was used, together with the general triple-ξ polarized basis set, namely the Def2-TZVP set from the EMSL Basis Set Exchange Library.[12] Such functionals and basis sets were chosen as the result of a systematic investigation of the geometry of various Cu^I and Ag^I model clusters carried out in our laboratory and comparison with experimental structures and post-HF calculations. Indeed, test calculations with various functionals indicate that the efficiency of DFT in treating d^{10}–d^{10} interactions is limited, even when dispersion corrections are included. On the other hand, although the BP86 functional is not designed for accounting accurately for such interactions, it provides among the best structural results on the investigated species for a reasonable computational demand. Moreover, one should keep in mind that these weak intramolecular d^{10}–d^{10} forces have very little effect on the cluster shapes and the bonding energies discussed in this paper. All stationary points were fully characterized as true minima via analytical frequency calculations. Geometries obtained from DFT calculations were used to perform natural orbital and Wiberg analysis by the NBO 5.0 program.[13] Drawings of molecular structures were done using the Molekel[14] and Avogadro programs.[15]

EXPERIMENTAL SECTION

Syntheses and Characterizations. *Reagents and General Procedures.* All chemicals were purchased from commercial sources and used as received. Solvents were purified following standard protocols. All reactions were carried out under an N_2 atmosphere by using standard Schlenk techniques. The preparations of $[Cu_8(X)\{E_2P(OR)_2\}_6](PF_6)$ (E = S, Se; R = Et, ^{i}Pr; X = H,[5b] Br[5a,d]) have been reported previously. The starting copper(I) complex, $[Cu(CH_3CN)_4]PF_6$,[16a] and the ligand, $[NH_4][Se_2P(O^iPr)_2]$,[16b] were prepared according to the literature methods, whereas $[NH_4][S_2P(OEt)_2]$ was obtained from Aldrich. Melting points were measured by using a Fargo MP-2D melting point apparatus. The elemental analyses were measured by using an Elementar vario EL III-CHNS elemental analyzer. Ambient-temperature NMR spectra were recorded on a Bruker Advance DPX300 FT-NMR spectrometer operating at 300 MHz for ^{1}H and 121.5 MHz for $^{31}P\{^1H\}$. The $^{31}P\{^1H\}$ and $^{77}Se\{^1H\}$ NMR are referenced externally against 85% H_3PO_4 (δ = 0 ppm) and PhSeSePh (δ = 463 ppm), respectively. The chemical shift (δ) and coupling constant (J) are reported in ppm and Hz, respectively.

Synthesis of $[Cu_7(H)\{S_2P(OEt)_2\}_6]$ ($\mathbf{1_H}$). Method A. To a solution of $[Cu(CH_3CN)_4]PF_6$ (0.133 g, 0.358 mmol) in 20 mL of $CHCl_3$ were added $[NH_4][S_2P(OEt)_2]$ (0.062 g, 0.308 mmol) and $NaBH_4$ (0.002 g, 0.051 mmol), and the mixture was stirred at room temperature for 1 h. It was then filtered to get rid of any solid, and the filtrate was evaporated to dryness under vacuum to give a yellow solid, which was washed with deionized water and dried under vacuum to obtain $[Cu_7(H)\{S_2P(OEt)_2\}_6]$ as a white powder. Yield: 0.094 g (81%). Mp: 134 °C dec. ^{1}H NMR (300 MHz, $CDCl_3$, δ, ppm): 1.35 (t, 36H, OCH_2CH_3), 3.51 (bs, 1H), 4.17 (m, 24H, OCH_2CH_3). $^{31}P\{^1H\}$ NMR (121.49 M Hz, $CDCl_3$, δ, ppm): 107.2 ppm. Anal. Calcd for $C_{24}H_{61}Cu_7O_{12}P_6S_{12}$: C, 18.51; H, 3.95. Found: C, 18.42; H, 4.39. ESI-MS (m/z): $[M + Cu]^+$ found (calcd) 1620.1 (1620.7).

Method B. The reaction mixture of $[Cu_8(H)\{S_2P(OEt)_2\}_6]PF_6$[1a] (0.250 g, 0.141 mmol) with $NaBH_4$ (0.003 g, 0.072 mmol) in 20 mL of chloroform was stirred at room temperature for 2 h under nitrogen. It was washed with deionized water followed by dichloromethane and dried under vacuum to give $[Cu_7(H)\{S_2P(OEt)_2\}_6]$ ($\mathbf{1_H}$) as a white powder. Yield: 83%.

Synthesis of $[Cu_7(D)\{S_2P(OEt)_2\}_6]$ ($\mathbf{1_D}$). This compound could be obtained via a procedure similar to that for $\mathbf{1_H}$ by using $NaBD_4$ instead of $NaBH_4$. Yield: 0.202 g (72%). Mp: 135 °C dec. Anal. Calcd for $C_{24}H_{60}DCu_7O_{12}P_6S_{12}$: C, 18.50; H, 4.01. Found: C, 18.46; H, 4.41. ^{1}H NMR (300 MHz, $CDCl_3$): 1.34 (t, 36H, OCH_2CH_3), 4.15 (m, 24H, OCH_2CH_3). ^{2}H NMR (46.1 MHz, $CHCl_3$): 3.50 (bs, 1D, 298 K). ^{31}P NMR (121.5 MHz, $CDCl_3$): 107.8 ppm.

*Synthesis of $[Cu_7(Br)\{Se_2P(O^iPr)_2\}_6]$ (**2**).* A mixture of $[Cu(CH_3CN)_4]PF_6$ (0.110 g, 0.29 mmol), $[NH_4][Se_2P(O^iPr)_2]$ (0.072 g, 0.22 mmol), and Bu_4NBr (0.013 g, 0.037 mmol) in the ratio 8:6:1 was stirred at room temperature for 30 min in CH_2Br_2 to afford $[Cu_8(Br)\{Se_2P(O^iPr)_2\}_6]PF_6$. Then $NaBH_4$ (0.002 g, 0.061 mmol) was added. After 2 h, the yellow solution was then filtered to get rid of any solids, and then the filtrate was passed through Al_2O_3 to remove the impurities, from which the colorless solution was produced. It was dried under vacuum to give $[Cu_7(Br)\{Se_2P(O^iPr)_2\}_6]$ as a white powder. Yield: 0.071 g (25%). ^{1}H NMR (300 MHz, $CDCl_3$, δ, ppm): 1.34 (d, 72H, $OCH(CH_3)_2$), 4.74 (m, 12H, $OCH(CH_3)_2$). $^{31}P\{^1H\}$ NMR (121.5 MHz, $CDCl_3$, δ, ppm): 74.7 ppm (J_{PSe} = 672 Hz). $^{77}Se\{^1H\}$ NMR ($CDCl_3$, δ, ppm): 6.7 (d, 12Se, $Se_2P(OR)_2$, J_{SeP} = 661 Hz). Anal. Calcd for $C_{36}H_{84}BrCu_7O_{12}P_6Se_{12}$: C, 18.27; H, 3.58. Found: C,18.64; H, 3.69. ESI-MS (m/z): $[M + Cu]^+$ found (calcd) 2428.9 (2428.8).

Procedures for Single-Crystal X-ray Crystallography. Crystals were mounted on the tips of glass fibers with epoxy resin. X-ray diffraction analyses of the crystals were performed on a Bruker APEX II CCD diffractometer using graphite-monochromated Mo Kα radiation (λ = 0.71073 Å). Data reduction was performed with SAINT,[17] which corrects for Lorentz and polarization effects. A multiscan absorption correction based on SADABS was applied.[18] Structures were solved by the use of direct methods, and the refinements were performed by least-squares methods on F^2 with the SHELXL-97 package,[19] incorporated in SHELXTL/PC V5.10.[20] Unfortunately, the copper framework in both structures displayed a disorder phenomenon which will be discussed thoroughly in the text below. All non-hydrogen atoms were refined anisotropically. H atom on the alkyl side chains were added at idealized positions, and the position of the central hydride in $\mathbf{1_H}$ was located from the Fourier synthesis and refined isotropically. Selected crystallographic data are given as follows. $\mathbf{1_H}$: $C_{24}H_{61}Cu_7O_{12}P_6S_{12}$, trigonal, space group $R\bar{3}$, a = 20.734(4) Å, b = 20.734(4) Å, c = 11.374(2) Å, α = 90°, β = 90°, γ = 120°, V = 4234.7(13) cm^3, Z = 3, T = 296(2) K, μ = 3.245 mm^{-1}, R_{int} = 0.0259, R1 = 0.0663, wR2(F^2) = 0.1817 ($I > 2\sigma(I)$). The goodness of fit on F^2 was 1.032. **2**: $C_{36}H_{84}BrCu_7O_{12}P_7Se_{12}$, trigonal, space group $R\bar{3}$, a = 22.467(5) Å, b = 22.467(5) Å, c = 12.533(3) Å, α = 90°, β = 90°, γ = 120°, V = 5479(3) cm^3, Z = 3, T = 296(2) K, μ = 8.700 mm^{-1}, R_{int} = 0.0471, R1 = 0.0499, wR2(F^2) = 0.1346 ($I > 2\sigma(I)$). The goodness of fit on F^2 was 1.072. CCDC 952366 ($\mathbf{1_H}$) and 952367 (**2**) contain supplementary crystallographic data for this paper.

HEPTANUCLEAR SPECIES

Structural Analysis of the Heptanuclear Species $[Cu_7(X)(E_2PH_2)_6]^q$ (E = S, Se; X = □ (Vacancy), q = +1; X = H, F, Cl, Br, q = 0; X = O, S, q = −1). Since both series of dithio and diseleno ligands provided similar results, we will only discuss the major structural data obtained for the dithio series in the following (see Table 1). The corresponding diseleno data are given in Table S1 (Supporting Information). In previous calculations we have shown that the optimized structures of the hydride-containing clusters $Cu_7(H)(S_2CNH_2)_6$ and $Ag_7(H)(E_2PH_2)_6$ (E = S, Se) reproduce the tricapped-tetrahedral experimental structures of $Cu_7(H)[S_2CR]_6$ (R = NPr$_2$, NEt$_2$, aza-15-crown-5) and $Ag_7(H)[E_2P(OR)_2]_6$ (E = S, Se; R = ^{i}Pr, Et).[8] The present calculations on $Cu_7(H)(S_2PH_2)_6$ also

dx.doi.org/10.1021/ic402207u | Inorg. Chem. 2013, 52, 13253−13262

Table 1. Relevant Computed Structural Data Corresponding to the Optimized Geometries of $[Cu_7(X)(S_2PH_2)_6]^q$ (X = □ (Vacancy), H, F, Cl, Br, O, S)

q	$[Cu_7(X)(S_2PH_2)_6]^q$	sym	Cu−Cu (Å)	Cu−X (Å)
+1	X = □	C_3	3 × 3.19	
			3 × 3.22	
			3 × 3.24	
			3 × 4.52	
			3 × 4.57	
0	X = H	C_3	3 × 2.63	1.77
			3 × 2.71	3 × 1.76
			3 × 2.73	3 × 2.69
			3 × 2.86	
			3 × 2.90	
	X = F	C_3	3 × 2.95	2.31
			3 × 3.00	3 × 2.38
			3 × 3.01	3 × 2.79
			3 × 4.29	
			3 × 4.36	
	X = Cl	C_3	3 × 3.03	2.60
			3 × 3.15	3 × 2.69
			3 × 3.16	3 × 2.73
			3 × 4.33	
			3 × 4.39	
	X = Br	C_3	3 × 3.06	2.72
			3 × 3.21	3 × 2.73
			3 × 3.22	3 × 2.79
			3 × 4.40	
			3 × 4.51	
−1	X = O	C_3	3 × 2.75	2.20
			3 × 2.80	3 × 2.01
			3 × 2.82	3 × 2.50
			3 × 2.90	
			3 × 3.74	
	X = S	C_3	3 × 2.71	2.38
			3 × 2.82	3 × 2.39
			3 × 2.86	3 × 2.48
			3 × 3.87	
			3 × 3.94	

reproduce this geometry ,with the hydride lying in the middle of a copper tetrahedron (see Figures 1 and 2 and Table 1).

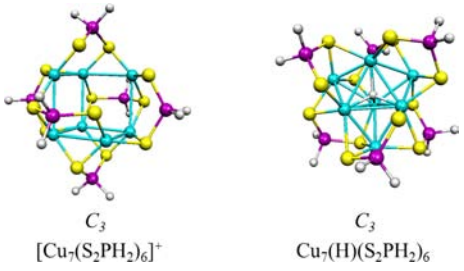

Figure 1. Optimized geometries of $[Cu_7(S_2PH_2)_6]^+$ and $Cu_7(H)(S_2PH_2)_6$.

With three Cu−H distances of 1.76 Å and one of 1.77 Å and bond angles of 109 and 110°, the hydride is clearly tetrahedrally coordinated, the three capping copper atoms lying far away (2.72 Å) from it. Removing the hydride from this model and reoptimizing the geometry of $[Cu_7(S_2PH_2)_6]^+$ leads to a structure of C_3 symmetry which can be described as a cube having a missing vertex (Figures 1 and 2 and Table 1). Thus,

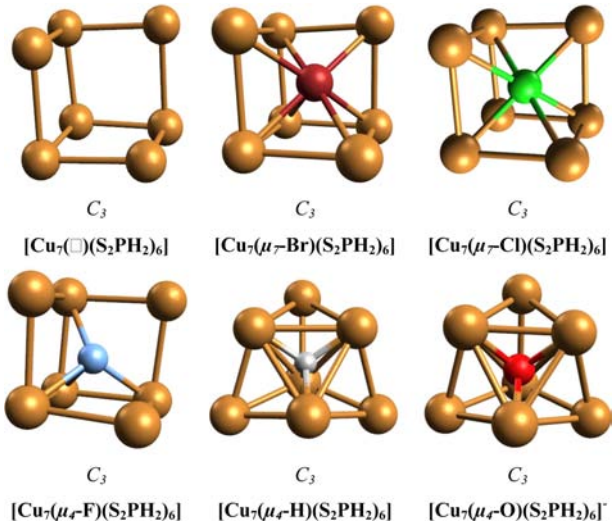

Figure 2. Cu_7X skeletons of some of the optimized heptanuclear models.

the tetrahedral distortion afforded when going from $[M^I]_8(E^{\cap}E)_6$ (cube) to $[M^I]_8(H)(E^{\cap}E)_6$ (tetracapped tetrahedron) is reproduced when going from $[M^I]_7(E^{\cap}E)_6$ (cube with a vacant vertex) to $M(I)_7(H)(E^{\cap}E)_6$ (tricapped tetrahedron). The same tetrahedral distortion is found when going from $[Cu_7(S_2PH_2)_6]^+$ to $[Cu_7(O)(S_2PH_2)_6]^-$ (optimized under C_3 symmetry), but it is less pronounced, as shown by the smaller relative difference between the four short Cu−O distances (2.01−2.20 Å) and the three long distances (2.50 Å). (Figure 2 and Table 1). A similar tendency for a moderate tetrahedral distortion was found in the octanuclear series for oxo-containing octanuclear species.[5c] It should be noted, however, that in $[Cu_7(O)(S_2PH_2)_6]^-$ the three metal atoms which are the closest to O are bonded to only two sulfur atoms, the third one lying now at a long nonbonding distance of 2.91 Å. Thus, in contrast to $Cu_7(H)(S_2PH_2)_6$, in $[Cu_7(O)(S_2PH_2)_6]^-$, all the S_2PH_2 ligands are μ_2,μ_1.

Whereas the fluoride-containing octanuclear species afford a weak tetrahedral distortion,[5c] this is not observed in the heptanuclear species. Indeed, the optimized structure of $Cu_7(F)(S_2PH_2)_6$ is best described as made up of a quite regular incomplete Cu_7 cube (one vacant vertex) with the encapsulated fluorine atom lying on the C_3 axis, not in the middle of the cube but shifted on the side opposite to the vacant vertex (Figure 2). In this situation, the encapsulated fluorine is not bonded to the same Cu atoms as in the tetrahedrally distorted $Cu_7(H)(E_2PH_2)_6$ or $[Cu_7(O)(E_2PH_2)_6]^-$ (except that on the C_3 axis) and lies in a trigonal umbrella-type configuration, with bond angles of 78 and 115° (Figure 2 and Table 1). The fact that in these heptanuclear clusters F is bonded differently from H and O to the copper atoms is likely due to the dominant ionic character of its bonding with the cage. Indeed, we have shown that, in addition to small size, the major driving force for a tetrahedral distortion in the octanuclear relatives is covalency.[5c] The weak covalent bonding existing in the case of fluorine is just strong enough to induce a small tetrahedral distortion on encapsulation in a Cu_8 cage, but not on encapsulation in a Cu_7 cage.

Synthesis and X-ray Structure of $[Cu_7(X)\{S_2P(O^iPr)_2\}_6]$ (X = H, Br). Clusters **1** and **2** have been characterized by single-crystal X-ray diffraction analyses. Compound $\mathbf{1}_H$ crystallized in

dx.doi.org/10.1021/ic402207u | Inorg. Chem. 2013, 52, 13253−13262

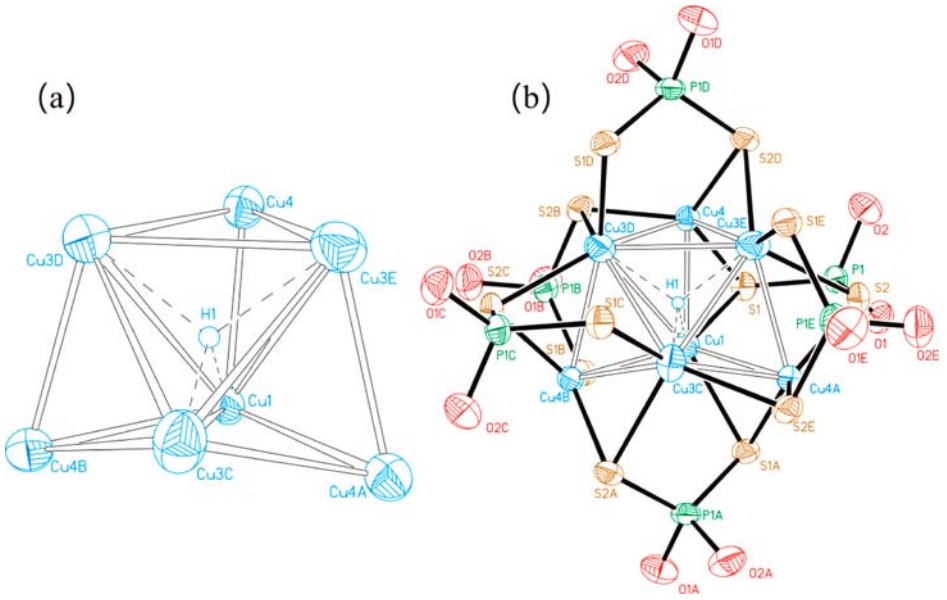

Figure 3. (a) Perspective view of the $[Cu_7(H)]$ core in $\mathbf{1_H}$ (30% displacement ellipsoids). (b) Thermal ellipsoid drawing of $[Cu_7(H)\{S_2P(OEt)_2\}_6]$ with ethoxy groups omitted for clarity. Selected bond lengths (Å) and angles (deg): Cu(1)−H(1), 1.766(5); Cu(3)−H(1), 1.847(2); Cu(3C)−Cu(4A), 2.667(2); Cu(1)···Cu(3C), 3.010(5); Cu(1)−Cu(4A), 2.623(3); Cu(1)−S(1), 2.444(2); Cu(3C)−S(2A), 2.523(2); Cu(4A)−S(2E), 2.222(2); Cu(1)−S(1)−Cu(4), 67.64(7); S(1)−P(1)−S(2), 118.02(10); P(1D)−S(2D), 1.994(3); P(1D)−S(1D), 2.000(2).

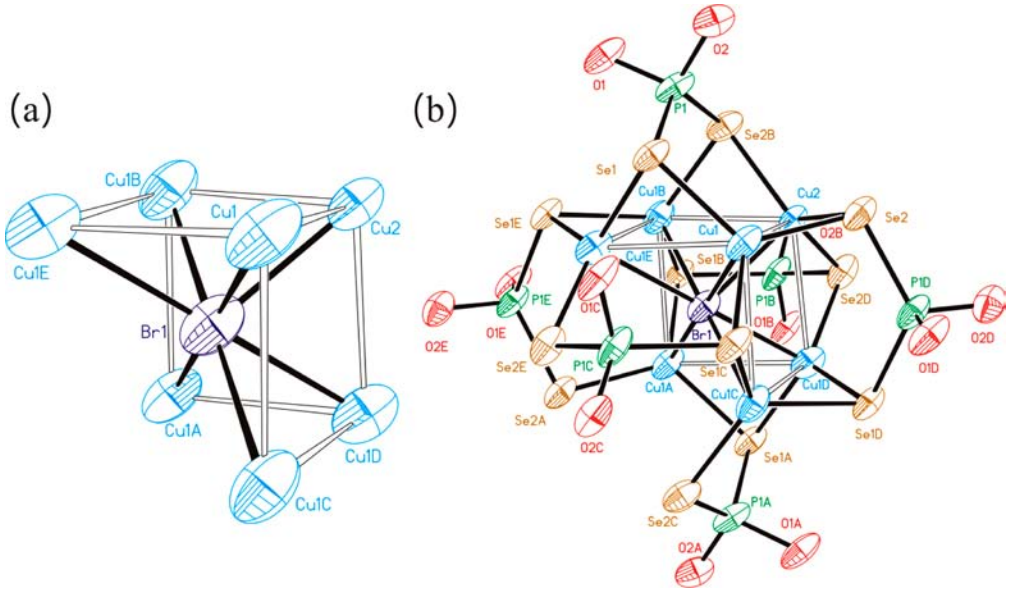

Figure 4. (a) Perspective view of the $[Cu_7(Br)]$ core in **2** (30% displacement ellipsoids). (b) Thermal ellipsoid drawing of $[Cu_7(Br)\{Se_2P(O^iPr)_2\}_6]$ with isopropyl groups omitted for clarity. Selected bond lengths (Å) and angles (deg): Cu(1)−Br(1), 2.574(4); Cu(2)−Br(1), 2.681(1); Cu(1)···Cu(2), 3.002(2); Cu(1)···Cu(1C), 3.128(2); Cu(1)···Cu(1E), 3.002(3); Cu(2)···Cu(1B), 3.001(2); Cu(1B)···Cu(1A), 3.000(2); Cu(1)−Se(2), 2.396(2); Cu(2)−Se(2), 2.413(2); Cu(1)−Br(1)−Cu(1C), 69.68(3); Cu(2)−Br(1)−Cu(1D), 71.44(3); Cu(1)−Se(2)−Cu(2), 76.94(5); Cu(1)−Se(1)−Cu(1E), 80.79(5).

the trigonal space group $R\bar{3}$, with three molecules in the unit cell. A total of 16 positions for seven copper atoms can be found in an atom array consisting of an inner and an outer cube. While the occupancy for each inner copper atom was fixed to be 50% ($0.5 \times 8 = 4$), it was calculated to be 10% for two Cu positions on the C_3 axis and 90% for the six Cu in general positions of the outer cube, which sum up to afford three Cu atoms. Overall the $Cu_7(H)$ core can be satisfactorily modeled as a hydride-centered tricapped tetrahedron as depicted in Figure 3a, whose copper skeleton is less distorted than the tricapped-triangular-pyramidal Cu_7 core observed in $Cu_7H(S_2CNPr_2)_6$.[8a] The edge lengths of the Cu_4 tetrahedron which consists of Cu1, Cu3C, Cu3D, and Cu3E (abbreviated as Cu_v) atoms lie in the range of 2.946(3)−3.010(5) Å. The Cu4 atom and its symmetry equivalents Cu4A and Cu4B are the three face-capping atoms, abbreviated as Cu_{cap}. Cu_v−Cu_{cap} bond lengths are in the range 2.623(3)−2.694(3) Å, slightly shorter than the sum of van der Waals radii of metallic copper, 2.80 Å.[21] The mean Cu_4−H distance (1.827(3) Å) is slightly longer than the 1.73 Å observed in the binary copper hydride, for which the hydride is four-coordinate.[22] The Cu_7H core is further inscribed within a distorted-icosahedral cage composed

dx.doi.org/10.1021/ic402207u | Inorg. Chem. 2013, 52, 13253−13262

Table 2. Relevant Bonding Parameters Computed for $[Cu_7(X)(S_2PH_2)_6]^q$ (X = H, F, Cl, Br, q = 0; X = O, S, q = −1)[a]

q	$[Cu_7(X)(S_2PH_2)_6]^q$	sym	BE (eV)	DE (eV)	ΔE_{Dist} (eV)	Cu−X Wiberg index	NAO net charge, population of X
0	X = H	C_3	8.84	7.71	1.13	1 × 0.129	−0.65, $1s^{1.64}$
						3 × 0.098	
						3 × 0.009	
	X = F	C_3	6.45	6.27	0.19	1 × 0.043	−0.86, $2s^{1.97}2p^{5.88}$
						3 × 0.040	
						3 × 0.015	
	X = Cl	C_3	5.04	4.82	0.21	1 × 0.073	−0.80, $3s^{1.95}3p^{5.83}$
						3 × 0.043	
						3 × 0.040	
	X = Br	C_3	4.55	4.25	0.30	1 × 0.081	−0.76, $4s^{1.95}4p^{5.80}$
						3 × 0.050	
						3 × 0.045	
−1	X = O	C_3	21.79	20.18	1.61	1 × 0.049	−1.66, $2s^{1.91}2p^{5.73}$
						3 × 0.118	
						3 × 0.034	
	X = S	C_3	16.39	15.29	1.10	1 × 0.162	−1.52, $3s^{1.86}3p^{5.60}3d^{0.04}$
						3 × 0.106	
						3 × 0.089	

[a]Legend: BE, bonding energy; DE, dissociation energy; ΔE_{Dist}, cage distortion energy. See text for definitions.

of 12 S atoms of the 6 diethyl dithiophosphate ligands (Figure 3b). While the CuS_3 coordination is revealed in each capping copper atom, it is CuS_3H that is identified on each vertex copper atom. Therefore, three of the six dithiophosphate ligands have a tetrametallic-tetraconnective (μ_2-S,μ_2-S) bonding mode. The other three exist in a trimetallic-triconnective (μ_2-S,μ_1-S) bridging pattern. The Cu−S bond lengths are in the range 2.219(3)−2.410(3) Å, and the S···S bite distances average 3.423(3) Å. Thus, as a whole, this crystal structure is fully consistent with that of the DFT-optimized $[Cu_7(H)(S_2PH_2)_6]$ model (see above).

The bromide-centered heptanuclear copper cluster of compound **2** also crystallized in the trigonal space group $R\bar{3}$, with three molecules in the unit cell. Because two copper atoms, Cu2 and Cu2A, on the crystallographic 3-fold axis are each 50% occupied, the conformation of seven copper atoms of **2** can be best described as a missing-corner cube with a bromide located at the center of inversion (Figure 4a). This is in sharp contrast to the geometry of the copper skeleton mentioned above, which displays a tricapped tetrahedron. The adjacent Cu···Cu distances are in the range 3.002(3)−3.128(2) Å, which are similar to the reported Cu···Cu distances (average 3.176 Å) in $[Cu_8(\mu_8\text{-Br})[Se_2P(O^iPr)_2]_6\}](PF_6)$.[5d] The Se−Cu distances in the range 2.396(2)−2.414(2) Å are comparable to those in $[Cu_8(\mu_8\text{-Br})\{Se_2P(O^iPr)_2\}_6](PF_6)$ (2.360(4)−2.438(4) Å), and the P−Se distances are in the range 2.163(2)−2.172(3) Å (average 2.16(8) Å). However, the Cu−Br distances ranging from 2.574(4) to 2.681(1) Å are shorter than those in $[Cu_8(\mu_8\text{-Br})\{Se_2P(O^iPr)_2\}_6]^+$ (2.73(2)−2.77(1) Å).[5d] The Cu−Br−Cu angles, 69.40(3)−71.97(3)°, are close to the value expected (70.53°) for a perfect centered cube. The Se···Se bite distance is 3.758(1) Å, and the Se−P−Se angle is 120.18(12)°. The Se−Cu−Se angles range from 116.58(3) to 121.72(6)°. Again, the molecular structure of **2** fits nicely with that predicted from the calculations on the $[Cu_7(Br)(S_2PH_2)_6]$ model (see above).

Cage-Anion Bonding Analysis within the Heptanuclear Series. We start the quantitative bonding analysis by considering the most relevant data computed for the $[Cu_7(X)(S_2PH_2)_6]^q$ series, which are reported in Table 2. The data corresponding to the $[Cu_7(X)(Se_2PH_2)_6]^q$ series (Table S2, Supporting Information) are quite similar and are therefore not discussed below. The dissociation energy (DE) is computed as the difference between the sum of the energies of X^{q-2} and of $[M_7(\square)(E_2PH_2)_6]^{2+}$ in its equilibrium geometry and the energy of $[M_7(X)(E_2PH_2)_6]^q$ in its equilibrium geometry. Although the computed DE has no real physical meaning, it constitutes a good qualitative tool for comparing the bonding within a series of anions having the same formal charge. The bonding energy (BE) is defined as the difference between the sum of the energies of X^{q-2} and the $[M_7(\square)(E_2PH_2)_6]^{2+}$ fragment in the frozen geometry it adopts in $[M_7(X)(E_2PH_2)_6]^{2+}$ and the energy of $[M_7(X)(E_2PH_2)_6]^q$ in its equilibrium geometry. For reasons similar to those for DEs, BEs can only be used for comparing series of clusters containing anions of the same charge. The difference between BE and DE (ΔE_{Dist}) is simply the amount of energy required for distorting the relaxed $[M_7(\square)(E_2PH_2)_6]^{2+}$ cage into the geometry it adopts in $[M_7(X)(E_2PH_2)_6]^q$. Thus, DE = BE − ΔE_{Dist}.

The lowest ΔE_{Dist} values are found for X = halogen, consistent with the fact that the encapsulation of these elements requires little contraction of the cage. For these elements, the covalent component of the bonding is weak, as shown by the NAO charges and Wiberg indices, from which one can sort the amount of covalency in the bonding as S > H > O > Br > Cl > F. In a previous study on anion encapsulation in the related series of octanuclear clusters, we have shown that the tetrahedral distortion afforded by the cage when encapsulating O^{2-} is associated with a strengthening of the participation of the 2s(O) orbital, whereas the 2p(O) participation is slightly decreased. Thus, the tetrahedral distortion is not associated with a tendency for sp^3 hybridization of the encapsulated oxygen. Taking into account that the more covalent sulfide and the smaller fluoride do not induce it, one can deduce that the tetrahedral distortion is the conjunction of both size and covalency effects.

dx.doi.org/10.1021/ic402207u | Inorg. Chem. 2013, 52, 13253−13262

Table 3. Relevant Computed Structural Data Corresponding to the Optimized Geometries of $[Cu_6(X)(S_2PH_2)_6]^{q-1}$ (X = □ (Vacancy), H, F, Cl, Br, O)

q	$[Cu_6(X)(S_2PH_2)_6]^q$	sym	Cu−Cu (Å)[a]	Cu−X (Å)	ligand coordination mode
0	X = □	S_6(A)	6 × 3.25		6 × μ_2,μ_1
		C_2	2 × 3.20; 2 × 3.23; 2 × 3.27		μ_2,μ_2; μ_1,μ_1; 4 × μ_2,μ_1
		C_s	7 × [2.79−3.40]		2 × μ_2,μ_2; 2 × μ_2,μ_1; μ_2,μ_0; μ_1,μ_1
		S_6(B)	6 × 3.53; 6 × 3.70		6 × μ_2,μ_1
−1	X = H	C_1 (close to C_2)	6 × [2.71−3.29];[b] 6 × [2.64−2.70][c]	1.73; 1.76; 1.77; 1.79; 2.88; 2.89	μ_2,μ_2; μ_1,μ_1; 4 × μ_2,μ_1
		S_6(B)	6 × 2.66; 6 × 2.73	6 × 1.90	6 × μ_2,μ_1
	X = F	C_3	3 × 2.93; 3 × 2.96	3 × 2.31; 3 × 2.62	
		S_6(B)	6 × 3.32; 6 × 3.42	6 × 2.38	
	X = Cl	S_6(A)	6 × 3.11	6 × 2.64	
		S_6(B)	6 × 3.45; 6 × 3.77	6 × 2.56	
	X = Br	S_6(A)	6 × 3.18	6 × 2.70	
		S_6(B)	6 × 3.52; 6 × 3.89	6 × 2.62	

[a]Shortest distances (see Figures 3 and 4). Values in brackets indicate ranges. [b]Core tetrahedron edges. [c]Cu(capping)−Cu(tetrahedron) distances.

Table 4. Relevant Bonding Parameters Computed for $[Cu_6(X)(S_2PH_2)_6]^q$ (X = H, F, Cl, Br, q = −1; X = O, S, q = −2)[a]

q	$[Cu_6(X)(S_2PH_2)_6]^q$	sym	E_R[b] (eV)	BE (eV)	DE (eV)	ΔE_{Dist} (eV)	Cu−X Wiberg index	NAO net charge, population of X
−1	X = H	C_1 (close to C_2)	0.34	6.25	4.84	1.41	0.169; 0.136; 0.092; 0.090; 0.013; 0.012	−0.60, $1s^{1.58}$
		S_6(B)	0.00	6.11	5.34	0.77	6 × 0075	−0.65, $1s^{1.63}$
	X = F	C_3	0.00	3.63	3.25	0.38	3 × 0.047; 3 × 0.023	−0.86, $2s^{1.97}2p^{5.89}$
		S_6(B)	0.08	3.78	3.54	0.24	6 × 0.034	−0.86, $2s^{1.97}2p^{5.89}$
	X = Cl	S_6(A)	0.00	2.21	1.90	0.31	6 × 0.054	−0.81, $3s^{1.95}3p^{5.84}$
		S_6(B)	0.53	2.19	1.75	0.44	6 × 0.056	−0.81, $3s^{1.94}3p^{5.84}$
	X = Br	S_6(A)	0.00	1.73	1.34	0.38	6 × 0.061	−0.77, $4s^{1.94}4p^{5.81}$
		S_6(B)	0.71	1.61	1.01	0.60	6 × 0.062	−0.77, $4s^{1.94}4p^{5.82}$

[a]Legend: BE, bonding energy; DE, dissociation energy; ΔE_{Dist}, cage distortion energy. See text for definitions. [b]Relative energy between isomers.

HEXANUCLEAR SPECIES

Structural Analysis of the Hexanuclear Species $[Cu_6(X)(E_2PH_2)_6]^{q-1}$ (E = S, Se; X = □ (Vacancy), q = 0; X = H, F, Cl, Br, q = −1). For the same reason as for the heptanuclear series, we only discuss in the following the structural results obtained for the dithio series (see Tables 3 and 4). The corresponding diseleno data are given in Tables S3 and S4 (Supporting Information). For obvious charge reasons, since the considered hexanuclear guest cages are now neutral, we only investigate their ability to encapsulate monoanions. We start the analysis in investigating the structure of the empty cage (X = □): i.e., $Cu_6(S_2PH_2)_6$.

In the same way as the $[Cu_7(S_2PH_2)_6]^+$ structure can be derived from that of $[Cu_8(S_2PH_2)_6]^{2+}$ by the removal of one Cu^+ atom on the metal cube (see above), it is possible to formally generate a $Cu_6(S_2PH_2)_6$ framework from $[Cu_8(S_2PH_2)_6]^{2+}$ by the removal of two Cu^+ atoms. There are actually three different ways for removing two vertices of a cube, leading to three different topologies, as sketched in Scheme 2. The two removed vertices can lie on the same edge of the cube (left), on the diagonal of a square face (middle), or on a solid diagonal of the cube (right). Viewing the parent cube as made of two interpenetrating identical tetrahedra (red and blue in Scheme 2), then the unique way to remove two vertices in preserving intact one of the tetrahedra corresponds to the C_2 configuration (see the complete red tetrahedron in middle of Scheme 2). This point will be discussed in more detail later.

The optimized geometries of the three $Cu_6(S_2PH_2)_6$ isomers are shown in Figure 5, together with their relative energies. Some relevant structural data are provided in Table 3. It turns out that the most stable isomer is that which derives from the cube by removing two vertices situated on a solid diagonal. The reason lies in the fact that, among the three structures, this is the most regular: that is, the only one which provides the same bonding mode to each of the six dithio ligands (μ_2,μ_1). To our knowledge, there is only one experimental structure of the type $Cu_6(E^{\cap}E)_6$ that is known so far: namely, $Cu_6[\{S_2P(OEt_2)\}]_6$.[4c,g,9a] It is interesting to note that it has the same structure as the S_6(A) isomer of the $Cu_6(E_2PH_2)_6$ model. One should note, however, that the two silver relatives which are known ($Ag_6[\{E_2P(O^iPr_2)\}]_6$, E = S,[9a] Se[4d]) exhibit a metal−ligand connectivity which cannot be derived from the topology of the $M^I_8(E^{\cap}E)_6$ cubic species, although the metal is also in a trigonal-planar environment. We have also optimized the $Cu_6(E_2PH_2)_6$ model assuming this geometry, which is of ideal

Scheme 2. The Three M_6 Frameworks That Can Be Formally Generated by Removing Two Metal Vertices from a Cubic Octanuclear $M_8(E^{\cap}E)_6$ Cluster[a]

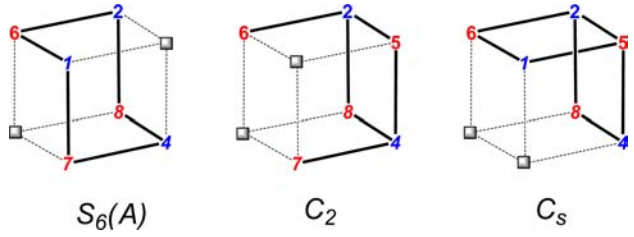

[a]The reported ideal symmetry groups are those of the full $M_6(E^{\cap}E)_6$ clusters.

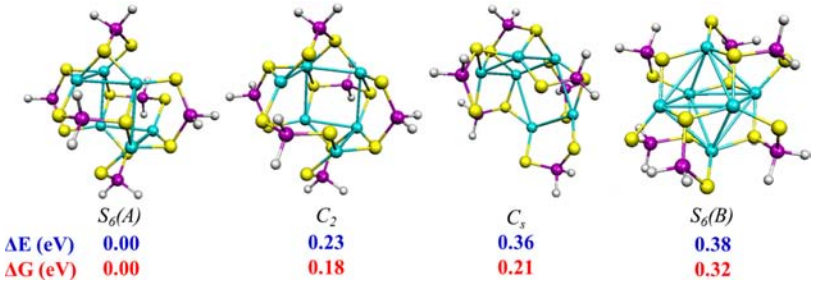

Figure 5. Optimized geometries of the three $Cu_6(S_2PH_2)_6$ isomers as defined in Scheme 2

D_{3d} symmetry. The energy minimum is found to be distorted to S_6 symmetry, due to a twisting motion of the E_2PH_2 ligands which allows them to relax their bite constraint. This minimum, denoted S_6(B), is less stable than the cube-generated S_6(A) minimum (see Figure 5).[23] Its Cu_6 framework can be viewed as an octahedron, but the Cu−Cu distances (3.53 and 3.70 Å) are on average longer than in the three other isomers (Table 3). Actually, the S_6(A) and the S_6(B) structure types are the only ones characterized[4c,d,g,9a,b] among quite a large number of possible distinct arrangements for $M_6(E^{\cap}E)_6$ (M = Cu^I, Ag^I; E = S, Se) clusters, all of them allowing local ME_3 trigonal-planar configurations with the six dichalcogeno ligands in a μ_2,μ_1 coordination mode.[9a,b] In this paper, we only investigated the encapsulating properties of the four isomers shown in Figure 5.

In the first stage, we investigated the possibility for the three cube-derived S_6(A), C_2, and C_s cages of Scheme 2 to encapsulate anions. In the case of $[Cu_6(H)(E_2PH_2)_6]^-$ the C_2 structure is found to be more stable than the C_s and S_6 structures (by 0.25 and 0.16 eV, respectively). The reason lies in the fact that this structure is the only one which preserves the existence of a Cu_4 tetrahedron (the red vertices in Scheme 2) within the Cu_6 framework and therefore allows the tetrahedral distortion. Indeed, the Cu_6H core of the optimized C_2 structure in $[Cu_6(H)(E_2PH_2)_6]^-$ can be described as a metallic bicapped tetrahedron, with the hydride sitting right in the middle of the bicapped tetrahedron. However, this C_2 structure is associated with a small imaginary frequency of b symmetry (30i cm^{-1}), indicating that it is not a true energy minimum at the considered level of calculations. The true minimum of C_1 symmetry was found to be more stable by only 0.06 eV. It still exhibits the hydride in the middle of a bicapped tetrahedron (Figure 6 and Table 3) and results from a small distortion away from the C_2 geometry, mainly associated with ligand relaxation. Incidentally, calculations on the hypothetical X = O model compound (not further discussed in this paper) lead also to a related tetrahedrally distorted structure.

In the case of the larger halides (Cl^- and Br^-), the encapsulated atom is hexacoordinated, and the encapsulating cage maintains its most stable S_6(A) structure. The same cubic derivation is found for F^-, for which the S_6(A) structure is more stable than the C_s and C_2 structures. However, this structure is not an energy minimum (one imaginary frequency, 47i cm^{-1} (a_u)). The true minimum (of C_3 symmetry) derives from it by a shifting of the fluorine atom along the C_3 axis, in such a way that it is now bonded to only three metal atoms in a flattened-pyramidal coordination mode (bond angles of 72 and 109°). Thus, one can say that the structure of the halide-containing hexanuclear species derives from those of their heptanuclear relatives by simply removing the Cu^+ atoms which lie on the C_3 axis.

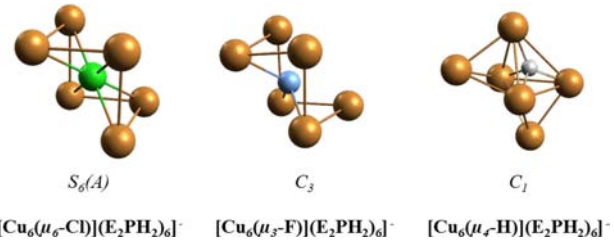

Figure 6. Cu_6X skeletons of some of the optimized hexanuclear models (see text).

We now move to the encapsulating ability of the S_6(B) guest cage. Energy minima of S_6 symmetry, i.e. with X lying in the middle of the Cu_6 octahedron, were found for all the tested anions. Only in the case of X = H was this structure found to be the most stable (see below). In general, the Cu−X distances were found somewhat larger in this S_6(B) configuration, indicating a lower flexibility of the S_6(B) guest cage, in comparison with the three other cube-derived cages of Figure 3.

Cage-Anion Bonding Analysis within the Hexanuclear Series. The most relevant bonding data computed for the $[Cu_6(X)(S_2PH_2)_6]^q$ series are given in Table 4. The data corresponding to the $[Cu_6(X)(Se_2PH_2)_6]^q$ series are provided in Table S4 (Supporting Information). We discuss first the encapsulation in the cube-derived cages (C_1 and S_6(A) structures). Consistent with the fact that the empty cage is neutral, the ionic component of its bonding with the encapsulated anion is weaker than in the heptanuclear series and the bonding energies are also weaker. Whereas in the case of X = halogen, the trends of the Cu−X Wiberg indices and NAO populations indicate no increase in the covalency on going from the hepta- to the hexanuclear cage, the opposite situation is found for X = H (compare Tables 2 and 4). This significant covalent interaction is favored by the tetrahedral distortion,[5c] which in turn induces the cluster cage to favor its less stable C_2 configuration (Figure 6). Looking now at the trends in the dissociation energies, it appears clear that the stabilities of the cube-derived hexanuclear anion-containing species are lower than those of their heptanuclear relatives. However, it should be noted that the DE value computed for $[Cu_6(H)(S_2PH_2)_6]^-$ is close to that found for $[Cu_7(X)(S_2PH_2)_6]$ (X = Cl, Br). Therefore, considering that we were able to prepare $[Cu_7(X)\{S_2P(O^iPr)_2\}_6]$ (X = Cl, Br) (see above), one can reasonably suggest that at least hydride-containing hexanuclear species of this type should be stable enough to be isolated.

Moving now to the S_6(B) structures, one can notice that in the case of X = H this structure is more stable than its C_1 isomer. This result is at variance with the case of the empty

dx.doi.org/10.1021/ic402207u | Inorg. Chem. 2013, 52, 13253−13262

Table 5. Bonding and Dissociation Energies Computed for $[Cu_8(X)(S_2PH_2)_6]^+$, $[Cu_7(X)(S_2PH_2)_6]$, and $[Cu_6(X)(S_2PH_2)_6]^-$ (X = H, Halogen)

	BE (eV)				DE (eV)			
	X = H	X = F	X = Cl	X = Br	X = H	X = F	X = Cl	X = Br
$[Cu_8(X)(S_2PH_2)_6]^+$ [a]	11.70	9.42	7.77	7.20	10.65	9.16	7.65	7.02
$[Cu_7(X)(S_2PH_2)_6]$	8.84	6.45	5.04	4.55	7.71	6.27	4.82	4.25
$[Cu_6(X)(S_2PH_2)_6]^-$ (S_6(A))	6.25	3.63	2.21	1.73	4.84	3.25	1.90	1.34

[a] From ref 5c.

cages (compare the C_2 and S_6(B) energies in Figure 5). This is due to a larger DE in the case of the hydride-containing S_6(B) isomer, which in turn results from a smaller ΔE_{Dist} value. In other words, the significant tetrahedral distortion of the C_2 guest cage requires more energy than the moderate cage contraction of the S_6(B) guest cage and it is not sufficiently balanced by a larger bonding energy resulting from the tetrahedral distortion. This larger bonding energy results from a larger covalent interaction, as can be seen from a comparison of the Wiberg indices and NAO populations (Table 4). On the other hand, simple net charge considerations indicate that the ionic interaction is weaker in the C_1 isomer.

In the case of X = halogen, the S_6(A) isomer is found to be the most stable. The major reason lies in the fact that the S_6(A) guest cage is largely more stable than the S_6(B) cage.

GENERAL CONSIDERATIONS

This work shows that DFT calculations can predict the stability and structure of subsequently characterized new species containing encapsulated elements, such as the heptanuclear compounds $[Cu_7(X)\{S_2P(O^iPr)_2\}_6]$ (X = Cl, Br). From our point of view, there is no reason to think that compounds of the type $[Cu_7(F)\{E_2P(OR)_2\}_6]$, and perhaps $[Cu_7(O)\{E_2P(OR)_2\}_6]^-$, or $[Cu_7(S)\{E_2P(OR)_2\}_6]^-$ (E = S, Se) should not be characterized. The encapsulating hexanuclear series might appear more hypothetical at first sight. One should note, however, that looking at the bonding and dissociation energies within the octa-, hepta-, and hexanuclear series of the computed cube-derived clusters (Table 5), the $[Cu_6(X)(S_2PH_2)_6]^-$ (X = H, F) clusters have BE and DE values of the same order of magnitude as those of the heptanuclear chlorine- and bromine-containing compounds, of which $[Cu_7(X)\{S_2P(O^iPr)_2\}_6]$ (X = Cl, Br) are real examples (see above).

Moreover, a related hydride-containing hexanuclear cluster, namely $[Cu_6(H)(TMTC)_3Cl_4]^+$ (TMTC = trimethyltriazacyclohexane), has been reported.[24] Its structure resembles that of our S_6(B) isomer. We have calculated, at the same level of theory, the BE and DE values on the simplified model $[Cu_6(H)(TC)_3Cl_4]^+$ (TC = triazacyclohexane), which has C_{3v} symmetry. These values (10.95 and 10.22 eV, respectively) are of the same order of magnitude as those reported in Table 1. Therefore, it is reasonable to believe that $[Cu_6(H)\{S_2P(OR)_2\}_6]^-$ compounds should be enough stable to be isolated.[25] For example, one may anticipate the S_6(A) structure generated from the $[Cu_7(H)\{S_2P(OR)_2\}_6]$ structure by removing a Cu(I) ion in the same way as $[Cu_7(H)\{S_2P(OR)_2\}_6]$ is generated from $[Cu_8(H)\{S_2P(OR)_2\}_6]^+$ by the removal of one Cu(I) ion (Scheme 1).

Finally we wish to mention that the formal continuous removal of metal vertices from an M_8 cube, in order to generate M_n species of lower nuclearity, does not stop at $n = 6$. Although no pentanuclear $M^I_5(E^{\cap}E)_6$ (M = d^{10}) species are known so far, tetranuclear complexes of the type $Zn^{II}_4(X)(E^{\cap}E)_6$ (X = O, S, Se) are well documented.[4i,26] The structures of these tetrahedral species can be derived from the octanuclear cubic species by removing the four blue vertices, as sketched in Scheme 3. In these compounds, the bonding between the oxide ion and its guest cage can be considered as localized, with an sp^3-hybridized oxygen and four tetrahedrally coordinated 18-electron metal centers.

Scheme 3. M_n (n = 8−4) Dichalcogenophosphate Cluster Cubic Derivation

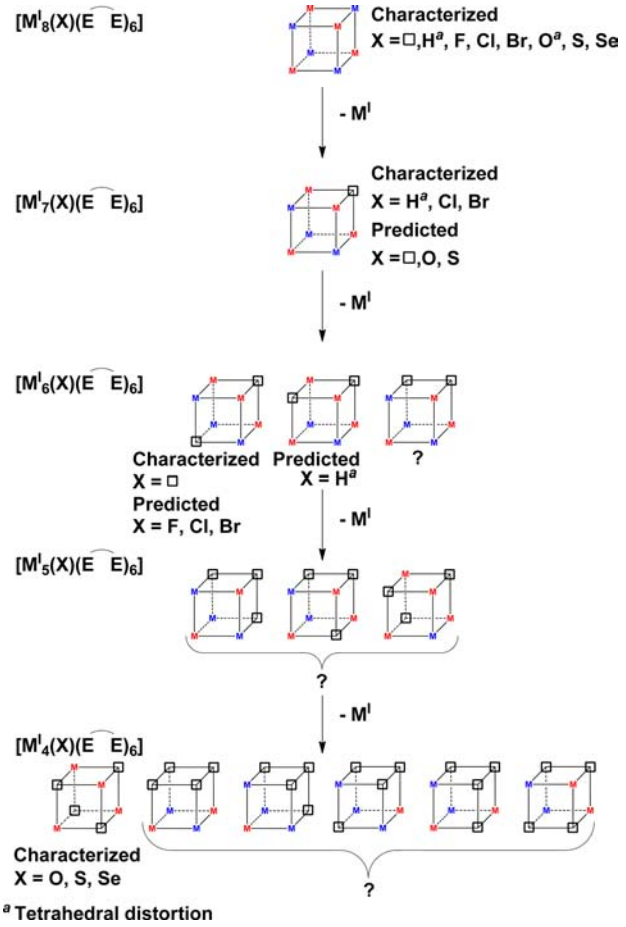

CONCLUSION

Theoretical investigations of hypothetical empty and anion-centered clusters of the type $[Cu^I]_7(X)(E^{\cap}E)_6$ and $[Cu^I]_6(X)(E^{\cap}E)_6$ (X = vacancy, H, or a main-group atom) indicate that several among these compounds are stable enough to be isolated. It turns out that we have already been able to synthesize two of the predicted heptanuclear species. Other

dx.doi.org/10.1021/ic402207u | Inorg. Chem. 2013, 52, 13253−13262

syntheses are in progress. The structure of most of the studied compounds can be derived from that of the octanuclear relatives $[Cu^{I}]_8(X)(E^{\frown}E)_6$ by formally removing one or two M(I) vertices of the metallic cube. Depending on the nature of the encapsulated anion, the cube-derived metallic cage affords or does not afford a distortion. With the largest third- and fourth-row anions, the cubic framework is maintained (with one or two vacant vertices). The smaller hydride and oxide anions induce a tetrahedral distortion. This tetrahedral distortion is not favored in the case of fluoride because of the lack of covalency in the host−guest bonding interaction. Rather, the cube-derived metallic arrangement is maintained and the fluoride is shifted away from the center of the cube in order to minimize the number of Cu−F bonds.

■ ASSOCIATED CONTENT

Ⓢ Supporting Information

Tables giving structural data and Cartesian coordinates for the computed optimized structures of hepta- and hexanuclear species and CIF files giving crystallographic data for $\mathbf{1}_H$ and **2**. This material is available free of charge via the Internet at http://pubs.acs.org.

■ AUTHOR INFORMATION

Corresponding Author

*E-mail for J.-Y.S.: saillard@univ-rennes1.fr.

Notes

The authors declare no competing financial interest.

■ ACKNOWLEDGMENTS

J.-Y.S. thanks the Institut universitaire de France for support. C.W.L. thanks the National Science Council of Taiwan (NSC 100-2113-M-259-003-MY3) for financial support.

■ REFERENCES

(1) (a) Lobana, T. S.; Wang, J.-C.; Liu, C. W. *Coord. Chem. Rev.* **2007**, *251*, 91−110. (b) Liu, C. W.; Woollins, J. D. In *Selenium and Tellurium Chemistry*; Woollins, J. D., Laitinen, R. S., Eds.; Springer-Verlag: Berlin, Heidelberg, 2011; Chapter 13, pp 303−320. (c) Haiduc, I. in *Handbook of Chalcogen Chemistry: New Perspectives in Sulfur, Selenium and Tellurium*; Devillanova, F. A., Ed.; RSC: Cambridge, U.K., 2006.

(2) Garland, M. T.; Halet, J.-F.; Saillard, J.-Y. *Inorg. Chem.* **2001**, *40*, 3342−3350.

(3) (a) Birker, P. J. M. W. L.; Freeman, H. C. *J. Am. Chem. Soc.* **1977**, *99*, 6890. (b) Birker, P. J. M. W. L. *Inorg. Chem.* **1979**, *18*, 3502. (c) Schugar, H. J.; Ou, C.-C.; Thich, J. A.; Potenza, J. A.; Felthouse, T. R.; Haddad, M. S.; Hendrickson, D. N.; Furey, W., Jr.; Lalancette, R. A. *Inorg. Chem.* **1980**, *19*, 543.

(4) (a) Wu, D.; Huang, J. Q.; Lin, Y.; Huang, J. L. *Sci. Sin. Ser. B (Engl. Ed.)* **1988**, *31*, 800. (b) Huang, Z. X.; Lu, S. F.; Huang, J. Q.; Wu, D. M.; Huang, J. L. *Jiegou Huaxue (J. Struct. Chem.)* **1991**, *10*, 213. (c) Liu, C. W.; Stubbs, T.; Staples, R. J.; Fackler, J. P., Jr. *J. Am. Chem. Soc.* **1995**, *117*, 9778. (d) Liu, C. W.; Shang, L.-J.; Wang, J.-C.; Keng, T.-C. *Chem. Commun.* **1999**, 995−996. (e) Liu, C. W.; Hung, C.-M.; Haia, H.-C; Liaw, B.-J.; Liou, L.-S.; Tsai, Y.-F.; Wang, J.-C. *Chem. Commun.* **2003**, 976−977. (f) Liu, C. W.; Hung, C.-M.; Santra, B. K.; Chen, H.-C.; Hsueh, H.-H.; Wang, J.-C. *Inorg. Chem.* **2003**, *42*, 3216−3220. (g) Liu, C. W.; Hung, C.-M.; Santra, B. K.; Wang, J.-C.; Kao, H.-M.; Lin, Z. *Inorg. Chem.* **2003**, *42*, 8551−8556. (h) Liu, C. W.; Haia, H.-C.; Hung, C.-M.; Santra, B. K.; Liaw, B.-J.; Lin, Z.; Wang, J.-C. *Inorg. Chem.* **2004**, *43*, 4464−4470. (i) Liu, C. W.; Irwin, M. D.; Mohamed, A. A.; Fackler, J. P., Jr. *Inorg. Chim. Acta* **2004**, *357*, 3950−3956.

(5) (a) Liu, C. W.; Sarkar, B.; Huang, Y.-J.; Liao, P.-K.; Wang, J.-C.; Saillard, J.-Y.; Kahlal, S. *J. Am. Chem. Soc.* **2009**, *131*, 11222−11233. (b) Liao, P.-K.; Sarkar, B.; Chang, H.-W.; Wang, J.-C.; Liu, C.-W. *Inorg. Chem.* **2009**, *48*, 4089−4097. (c) Latouche, C.; Kahlal, S.; Furet, E.; Liao, P.-K.; Lin, Y.-R.; Fang, C.-S.; Cuny, J.; Liu, C. W.; Saillard, J.-Y. *Inorg. Chem.* **2013**, *52*, 7752−7765. (d) Liu, C. W.; Hung, C.-M.; Santra, B. K.; Chu, Y.-H.; Wang, J.-C.; Lin, Z. *Inorg. Chem.* **2004**, *43*, 4306−4314.

(6) (a) Liu, C. W.; Chang, H.-W.; Sarkar, B.; Saillard, J.-Y.; Kahlal, S.; Wu, Y.-Y. *Inorg. Chem.* **2010**, *49*, 468−475. (b) Liu, C. W.; Chang, H.-W.; Fang, C.-S.; Sarkar, B.; Wang, J.-C. *Chem. Commun.* **2010**, *46*, 4571−4573.

(7) (a) Liao, P.-K.; Liu, K.-G.; Fang, C.-S.; Liu, C. W.; Fackler, J. P., Jr.; Wu, Y.-Y. *Inorg. Chem.* **2011**, *50*, 8410−8417. (b) Liao, P.-K.; Shi, D.-R.; Liao, J.-H.; Liu, C. W.; Artem'ev, A. V.; Kuimov, V. A.; Gusarova, N. K.; Trofimov, B. A. *Eur. J. Inorg. Chem.* **2012**, *30*, 4921−4929.

(8) (a) Liao, P.-K.; Fang, C.-S.; Edwards, A. J.; Kahlal, S.; Saillard, J.-Y.; Liu, C. W. *Inorg. Chem.* **2012**, *51*, 6577−6591. (b) Liu, C. W.; Lin, Y.-R.; Fang, C.-S.; Latouche, C.; Kahlal, S.; Saillard, J.-Y. *Inorg. Chem.* **2013**, *52*, 2070−2077.

(9) (a) Liu, C. W.; Pitts, J. T.; Fackler, J. P., Jr. *Polyhedron* **1997**, *16*, 3899. (b) Fackler, J. P., Jr.; Staples, R. J.; Liu, C. W.; Stubbs, R. T.; Lopez, C.; Pitts, J. T. *J. Pure Appl. Chem.* **1998**, *70*, 839. (c) Liu, C. W.; Staples, R. J.; Fackler, J. P., Jr. *Coord. Chem. Rev.* **1998**, *174*, 147−177.

(10) Frisch, M. J.; Trucks, G. W.; Schlegel, H. B.; Scuseria, G. E.; Robb, M. A.; Cheeseman, J.; Scalmani, G.; Barone, V.; Mennucci, B.; Petersson, G. A.; Nakatsuji, H.; Caricato, M.; Li, X.; Hratchian, H. P.; Izmaylov, A. F.; Bloino, J.; Zheng, G.; Sonnenberg, J. L.; Hada, M.; Ehara, M.; Toyota, K.; Fukuda, R.; Hasegawa, J.; Ishida, M.; Nakajima, T.; Honda, Y.; Kitao, O.; Nakai, H.; Vreven, T.; Montgomery, J. A., Jr.; Peralta, J. E.; Ogliaro, F.; Bearpark, M.; Heyd, J. J.; Brothers, E.; Kudin, K. N.; Staroverov, V. N.; Kobayashi, R.; Normand, J.; Raghavachari, K.; Rendell, A.; Burant, J. C.; Iyengar, S. S.; Tomasi, J.; Cossi, M.; Rega, N.; Millam, J. M.; Klene, M.; Knox, J. E.; Cross, J. B.; Bakken, V.; Adamo, C.; Jaramillo, J.; Gomperts, R.; Stratmann, R. E.; Yazyev, O.; Austin, A. J.; Cammi, R.; Pomelli, C.; Ochterski, J. W.; Martin, R. L.; Morokuma, K.; Zakrzewski, V. G.; Voth, G. A.; P, S.; Dannenberg, J. J.; Dapprich, S.; Daniels, A. D.; Farkas, O.; Foresman, J. B.; Ortiz, J. V.; Cioslowski, J.; Fox, D. J. *Gaussian 09, revision A.02*; Gaussian, Inc., Wallingford, CT, 2009.

(11) (a) Becke, A. D. *Phys. Rev. A* **1988**, *38*, 3098−30100. (b) Perdew, J. P. *Phys. Rev. B* **1986**, *33*, 8822−8824.

(12) Weigend, F.; Ahlrichs, R. *Phys. Chem. Chem. Phys.* **2005**, *7*, 3297−3305.

(13) Glendening, E. D.; Badenhoop, J. K.; Reed, A. E.; Carpenter, J. E.; Bohmann, J. A.; Morales, C. M.; Weinhold, F. *NBO 5.0*; Theoretical Chemistry Institute, University of Wisconsin, Madison, WI, 2001; http://www.chem.wisc.edu/ ∼ nbo5.

(14) Flükiger, P.; Lüthi, H. P.; Portmann, S.; Weber, J. *Molekel 4.3*; Swiss Center for Scientific Computing, Manno, Switzerland, 2000−2002; http://www.cscs.ch/molkel/.

(15) Hanwell, M. D.; Curtis, D. E.; Vandermeersch, T.; Zurek, E.; Hutchison, G. R. *J. Cheminf.* **2012**, *4*, 17.

(16) (a) Kubas, G. J. *Inorg. Synth.* **1979**, *19*, 90. (b) Liu, C. W.; Shang, I.-J.; Hung, C.-M.; Wang, J.-C.; Keng, T.-C. *Dalton Trans.* **2002**, 1974−1979.

(17) *SAINT V4.043: Software for the CCDC Detector System*; Bruker Analystic X-ray Systems, Madison, WI, 1995.

(18) Sheldrick, G. M. *SADABS*; University of Gottingen, Gottingen, Germany, 1996.

(19) Sheldrick, G. M. *Acta Crystallogr.* **2008**, *A64*, 112−122.

(20) *SHELXL 5.10 (PC version): Program Library for Structure Solution and molecular Graphics*; Bruker Analytical X-ray Systems, Madison, WI, 1998.

(21) Bondi, A. *J. Phys. Chem.* **1964**, *68*, 441−451.

(22) Goedkoop, J. A.; Anderson, A. F. *Acta Crystallogr.* **1955**, *8*, 118−119.

(23) Preliminary calculations on the silver relative found both S_6 isomers to be almost isoenergetic at the same level of theory.
(24) Köhn, R. D.; Pan, Z.; Mahon, M. F.; Kociok-Köhn, G. *Chem. Commun.* **2003**, 1272−1273.
(25) Hoffmann, R.; Schleyer, P. v. R.; Schaefer, H. F., III *Angew. Chem., Int. Ed.* **2008**, *47*, 7164−7167.
(26) (a) Harrison, P. G.; Begley, M. J.; Kikabhai, T.; Killer, F. *J. Chem. Soc., Dalton Trans.* **1986**, 925. (b) Albinati, A.; Casarin, M.; Maccato, C.; Pandolfo, L.; Vittadini, A. *Inorg. Chem.* **1999**, *38*, 1145. (c) Santra, B. K.; Hung, C.-M.; Liaw, B.-J.; Wang, J.-C.; Liu, C. W. *Inorg. Chem.* **2004**, *43*, 7570−7572. (d) Liu, C. W.; Lobana, T. S.; Santra, B. K.; Hung, C.-M.; Liu, H.-Y.; Liaw, J.; Wang, J.-C. *Dalton Trans.* **2006**, 560.